chemistry

MDPI

Article

Surface Thermodynamic Properties of Styrene–Divinylbenzene Copolymer Modified by Supramolecular Structure of Melamine Using Inverse Gas Chromatography

Tayssir Hamieh [1,2,*] **and Vladimir Yu Gus'kov** [3]

[1] Faculty of Science and Engineering, Maastricht University, P.O. Box 616, 6200 MD Maastricht, The Netherlands
[2] Laboratory of Materials, Catalysis, Environment and Analytical Methods (MCEMA), Faculty of Sciences, Lebanese University, Beirut P.O. Box 6573/14, Lebanon
[3] Faculty of Science and Technology, Ufa University of Science and Technology, P.O. Box 450076 Ufa, Russia; guscov@mail.ru
* Correspondence: t.hamieh@maastrichtuniversity.nl

Abstract: The surface thermodynamic properties of polymers and copolymers modified by supramolecular structures are used in several industrial processes, such as selective adsorption, paints, coatings, colloids, and adhesion applications. Background: Inverse gas chromatography at infinite dilution was proved to be the best technique to determine the surface properties of solid surfaces by studying the adsorption of some model polar and non-polar organic molecules adsorbed on solid surfaces at different temperatures. Methods: The retention volume of adsorbed solvents is a valuable parameter that was used to obtain the London dispersive and polar free energies and the London dispersive surface energy of styrene–divinylbenzene copolymer modified by supramolecular structure of melamine using both the Hamieh thermal model and our new methodology consisting of the separation of the two polar molecules and the dispersive free energy of their interaction. This led to the determination of the polar acid and base surface energy, and the Lewis acid–base constants of the various solid materials. Results: Following our new methodology, all surface energetic properties of styrene–divinylbenzene copolymer modified by melamine at different percentages were determined as a function of temperature. Conclusions: It was observed that the styrene–divinylbenzene copolymer exhibited the highest London dispersive surface energy, which decreased when the melamine percentage increased. All materials presented higher Lewis basicity and this Lewis basicity increased with the percentage of melamine.

Keywords: Hamieh thermal model; dispersive and polar free energy; thermal conductivity; London dispersive surface energy; Lewis acid–base parameters; polar acid–base surface energy; intermolecular separation distance; supramolecular structure

check for updates

Citation: Hamieh, T.; Gus'kov, V.Y. Surface Thermodynamic Properties of Styrene–Divinylbenzene Copolymer Modified by Supramolecular Structure of Melamine Using Inverse Gas Chromatography. *Chemistry* **2024**, *6*, 830–851. https://doi.org/10.3390/chemistry6050050

Academic Editor: Matthias Lehmann

Received: 16 July 2024
Revised: 22 August 2024
Accepted: 27 August 2024
Published: 30 August 2024

1. Introduction

Due to their important applications in the domain of molecular recognition and surface chemistry, in the last thirty years, several papers have been devoted to two-dimensional network supramolecular structures [1–16]. When supported on solid surfaces, these heterocyclic compounds, such as melamine, cyanuric acid, and uracil and its derivatives, are likely to constitute supramolecular network structures capable of selectively adsorbing various molecules, including enantiomers [10].

In the case of formed supramolecular structures on the surface of inert supports and porous polymer sorbents, it has been shown that the properties of the resulting adsorbents depend on the polarity of the surface and porosity of the initial adsorbents [1–16]. The effect of the amount of the supported modifier on the properties of the obtained adsorbents was studied by Sukhareva et al. [3] and Guskov et al. [10–16] using the inverse gas chromatography technique. They studied the specific interactions between the various polymer adsorbents and some model organic solvents, as well as the London dispersive energy of the various solid surfaces using the Dorris–Gray method [17]. It was proved in other works that the classic chromatographic methods, such as that proposed by Schultz et al. [18], and the Dorris-Gray method, cannot be used for an accurate evaluation of the London dispersive surface energy of solid materials, because these methods were based on the hypothesis of the constant surface area of organic solvents. In several studies [19–23], an important effect of temperature on the surface area of organic molecules was highlighted and more accurate values of the London dispersive and polar components of the surface energy, and the Lewis acid–base properties of various solid substrates were obtained using the Hamieh thermal model. Furthermore, the polar and dispersive interactions between the organic solvents and several solid surfaces were determined by applying the new method [24,25] using the London interaction equation [26].

In this paper, we were interested in the determination of the surface thermodynamic properties of some important porous polymers such as styrene–divinylbenzene copolymer modified by the supramolecular structure of melamine. Indeed, the highly porous structure, chemical stability, easier functionalization, and large surface area of this copolymer make it an excellent candidate for several applications such as biotechnology, environmental science, industrial chemistry, adsorption, and catalysis.

Inverse gas chromatography (IGC) at infinite dilution [27–40] was used in applying our new methodology, which consisted of the correction of the London dispersive surface energy and the correct determination of polar free energy of adsorption of some polar organic probes, as well as the Lewis acid–base parameters of the modified porous polymer.

2. Materials and Methods

2.1. Adsorbent and Materials

A porous polymer such as styrene–divinylbenzene copolymer (Dowex L-285, from Dow Chemical, Midland, MI, USA), was used as the initial adsorbent for modification. Its specific surface area was 800 m^2/g, with particle sizes of 250–500 µm. The chosen surface modifier was melamine (from Vecton, St. Petersburg, Russia, 97%, CAS108-78-1), with percentage mass from 1% to 4%, impregnated into the adsorbent surface by evaporation of aqueous solutions at 60 °C. The amount of melamine necessary for coating the adsorbent surface with a monolayer was determined from the specific surface area of the sorbent and molecular dimensions of melamine. The surface area of the melamine molecule was previously determined and shown to be equal to 139.8 $Å^2$ [3]. This allowed us to determine the various melamine percentages needed for the formation of the planar layer of the supramolecular structure of melamine. The temperature choice was necessary to uniformly impregnate the modifier on the surface. Then, the resulting sample was washed with high-purity water to pH 7. Chemically pure organic solvents such as *n*-hexane, *n*-heptane, *n*-octane, benzene, cyclohexane, toluene, ethanol, *n*-propanol, *n*-butanol, *i*-propanol, *i*-butanol, n-pentanol, i-pentanol, dichloromethane, and ethyl acetate (Chimreactivsnab, Russia) were used as the probes.

2.2. Inverse Gas Chromatography

The experimental determination of the retention time of organic molecules adsorbed on Dowex L-285 was carried out using inverse gas chromatography at infinite dilution with the help of a Chromos GC-1000 chromatograph (from Chromos, Russia) equipped with a flame ionization detector (FID). The solid particles were packed into stainless steel columns of 30 cm length and 3 mm internal diameter. The temperature of the column was 200 °C and the temperatures of the injector and detector were 280°C. The flow rate of the nitrogen carrier gas was 30 mL/min. The mass of the sorbent packed into the column was equal to 1 g. All chromatographic columns were conditioned overnight at 200 °C to remove any residual impurities. The probes in the vapor phase were injected with microsyringes at different temperatures to realize the infinite dilution and to satisfy Henry's law. The experiments were repeated three times and the error in the value of the retention volume did not exceed 2%.

2.3. Thermodynamic Methods

2.3.1. Dispersive and Polar Energies, and Lewis Acid–Base Parameters

The chromatographic measurements led to the determination of the net retention volume Vn of the different probes adsorbed on the solid surfaces. This allowed determination of the values of the free energy of adsorption ΔG_a^0 of the adsorbed organic molecules as a function of temperature using the following equation:

$$\Delta G_a^0(T) = -RTlnVn + C(T) \tag{1}$$

where T is the absolute temperature, R the perfect constant gas, and $C(T)$ a constant depending on the temperature and the solvent–sorbent interaction.

In the case of non-polar probes such as n-alkanes, $\Delta G_a^0(T)$ is equivalent to the London dispersive energy $\Delta G_a^d(T)$ of adsorption for all temperatures:

$$\Delta G_a^0(T) = \Delta G_a^d(T) \tag{2}$$

When polar molecules are adsorbed on solid materials, $\Delta G_a^0(T)$ is written as follows:

$$\Delta G_a^0(T) = \Delta G_a^d(T) + \Delta G_a^p(T) \tag{3}$$

where $\Delta G_a^{sp}(T)$ is the free polar energy of the polar solvents.

To separate the two dispersive and polar contributions of the free energy of adsorption, we applied the new methodology recently published [24,25] that used the London dispersion interaction energy Equation (4):

$$\Delta G_a^d(T) = -\frac{\alpha_{0S}}{H^6}\left[\frac{3\mathcal{N}}{2(4\pi\varepsilon_0)^2}\left(\frac{\varepsilon_S\,\varepsilon_X}{(\varepsilon_S+\varepsilon_X)}\alpha_{0X}\right)\right] \tag{4}$$

where $\mathcal{N}$ is the Avogadro number, ε_0 the dielectric constant of vacuum, α_{0S} and α_{0X} are the respective deformation polarizabilities of the solid material denoted by S and the organic molecule denoted by X, separated by a distance H, and ε_S and ε_X are their corresponding ionization energies.

Previous equations led to Equation (5):

$$RTlnVn = \frac{\alpha_{0S}}{H^6}\left[\frac{3\mathcal{N}}{2(4\pi\varepsilon_0)^2}\left(\frac{\varepsilon_S\,\varepsilon_X}{(\varepsilon_S+\varepsilon_X)}\alpha_{0X}\right)\right] - \Delta G_a^p(T) + C(T) \tag{5}$$

The new chosen chromatographic interaction parameter $\mathcal{P}_{SX}$ was given by

$$\mathcal{P}_{SX} = \frac{\varepsilon_S\,\varepsilon_X}{(\varepsilon_S+\varepsilon_X)}\alpha_{0X} \tag{6}$$

For non-polar molecules such as n-alkanes, the representation of $RTlnVn$ of these molecules is given by

$$\begin{cases} RTlnVn(non-polar) = A\left[\frac{3\mathcal{N}}{2(4\pi\varepsilon_0)^2}\mathcal{P}_{SX}(non-polar)\right] + C(T) \\ A = \frac{\alpha_{0S}}{H^6} \end{cases} \tag{7}$$

where A is the slope of the non-polar straight line.

Using the distance between the straight line of n-alkanes and the representative point of a polar molecule, it was possible to determine the free polar energy $\Delta G_a^p(polar)$ of the polar molecule, at any temperature:

$$\Delta G_a^p(T,\ polar) = RTlnVn\ (T,\ polar) - A\left[\frac{3\mathcal{N}}{2(4\pi\varepsilon_0)^2}\mathcal{P}_{SX}(polar)\right] - C(T) \tag{8}$$

The polar enthalpy $\left(-\Delta H_a^p\right)$ and entropy $\left(-\Delta S_a^p\right)$ of polar probes adsorbed on porous polymers can be deduced from Equation (9) if the linearity of $\Delta G_a^p(T)$ is assured:

$$\Delta G_a^p(T) = \Delta H_a^p - T\Delta S_a^p \tag{9}$$

The Lewis acid–base properties of the solid substrates characterized by its enthalpic (K_A, K_D) and entropic (ω_A, ω_D) acid–base constants are obtained:

$$\begin{cases} (-\Delta H^p) = \ K_A \times DN' + K_D \times AN' \\ \left(-\Delta S_a^p\right) = \omega_A \times DN' + \omega_D \times AN' \end{cases} \tag{10}$$

where DN' and AN' are, respectively, the corrected electron donor and acceptor numbers of the polar molecule [41,42].

2.3.2. London Dispersive Surface Energy, and Lewis Acid–Base Surface Energies

The London dispersive surface energy $\gamma_s^d(T)$ of the different sorbents was determined using the Fowkes relation [43] and applying the Hamieh thermal model that gave the surface area $a(T)$ of organic molecules as a function of the temperature [19–23]:

$$RTlnV_n = 2\mathcal{N}a(T)\left(\gamma_l^d\gamma_s^d\right)^{1/2} + \beta(T) \tag{11}$$

where $\beta(T)$ is a constant depending only on the temperature and the solid material.

The total surface energy of material is then given by

$$\gamma_s = \gamma_s^d + \gamma_s^p \tag{12}$$

where γ_s^p represents the total polar (or acid–base) contribution of the surface energy.

Using Van Oss et al.'s method [44], it was possible to determine γ_s^p of the different polymers. This method consists of the determination of the Lewis acid γ_s^+ and base γ_s^- surface energies of the solid particles. By choosing two monopolar solvents such as ethyl acetate (B) and dichloromethane (A), characterized by the following parameters:

$$\begin{cases} \gamma_A^+ = 5.2\ \mathrm{mJ/m^2},\ \gamma_A^- = 0 \\ \gamma_B^+ = 0\ ,\ \gamma_B^- = 19.2\ \mathrm{mJ/m^2} \end{cases} \tag{13}$$

and using the expression of polar free energy $\Delta G_a^p(T)$ of the polar molecules, given by Equation (14):

$$\Delta G_a^p(T) = 2\mathcal{N}a(T)\left(\sqrt{\gamma_l^-\gamma_s^+} + \sqrt{\gamma_l^+\gamma_s^-}\right) \tag{14}$$

the Lewis acid and base surface energies of the solid surfaces were deduced from Equation (15):

$$\begin{cases} \gamma_s^+(\mathrm{T}) & = \dfrac{\left[\Delta G_a^p(T)(B)\right]^2}{4\mathcal{N}^2[a_B(T)]^2\gamma_B^-} \\ \gamma_s^-(\mathrm{T}) & = \dfrac{\left[\Delta G_a^p(T)(A)\right]^2}{4\mathcal{N}^2[a_A(T)]^2\gamma_A^+} \end{cases} \tag{15}$$

The polar (or acid–base) surface energy $\gamma_s^p = \gamma_s^{AB}$ and the total surface energy $\gamma_s^{tot.}$ of different materials were then obtained using Equation (16):

$$\begin{cases} \gamma_s^{AB} = 2\sqrt{\gamma_s^+ \gamma_s^-} \\ \gamma_s^{tot.} = \gamma_s^d + \gamma_s^{AB} \end{cases} \tag{16}$$

3. Results

3.1. Variations in $RTlnV_n(T)$ of Adsorbed Probes Against the Temperature

The experimental determination of the net retention volume V_n of organic molecules adsorbed on Dowex L-285 modified by different percentages of melamine as a function of temperature T led to the variations, with temperature, in $RTlnV_n(T)$ for the various organic solvents (Table S1). Using the obtained results, Figure 1 shows the curves of $RTlnV_n(T)$ of the different organic molecules at different temperatures, as well as the variations in $\Delta G_a(\text{-}CH_2\text{-})$ of n-alkanes adsorbed solid materials as a function of temperature.

where

$$\Delta G_a(\text{-}CH_2\text{-}) = RTln\frac{V_n(C_{n+1}H_{2n+4})}{V_n(C_nH_{2n+2})} \tag{17}$$

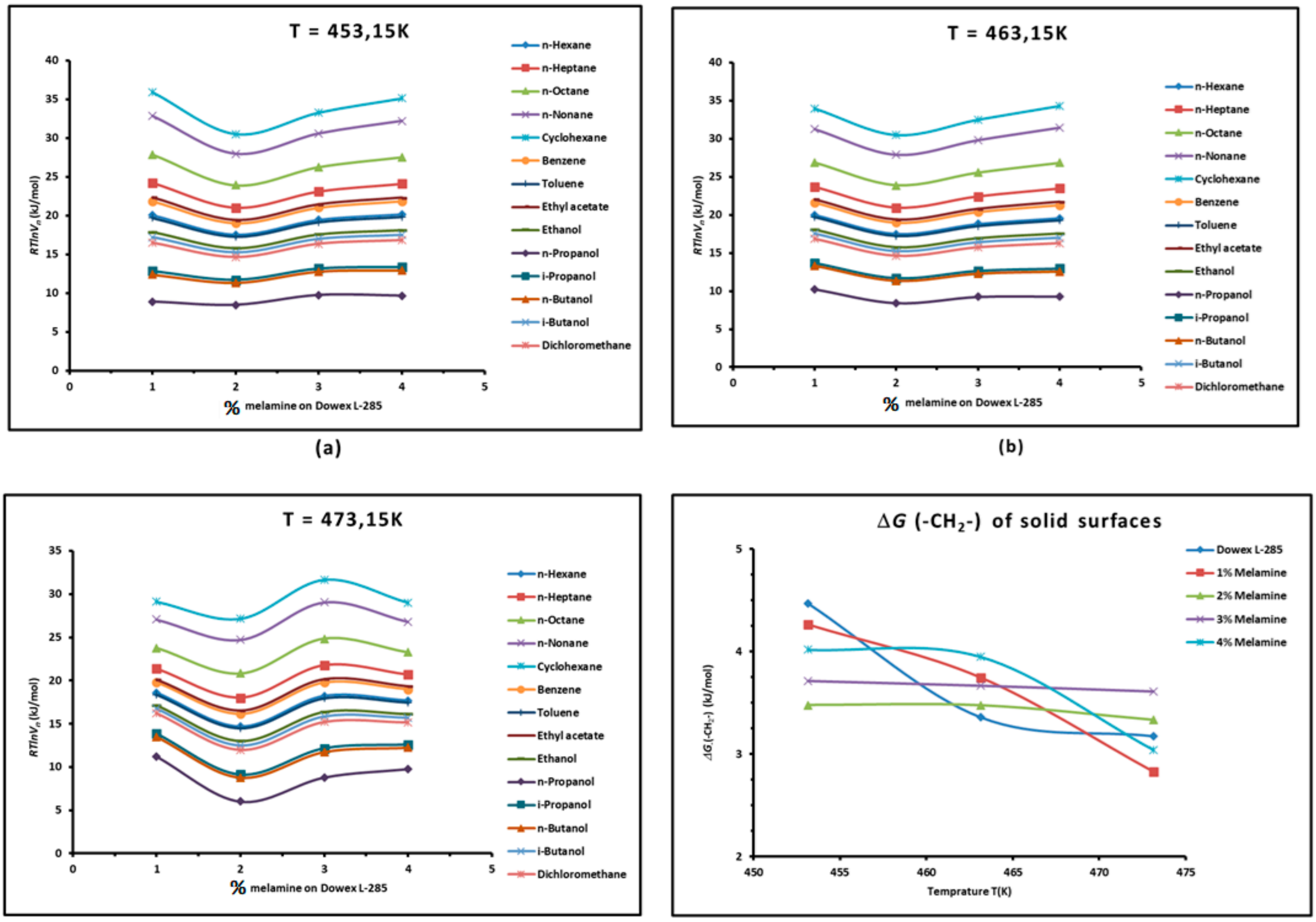

(a) (b)

(c) (d)

Figure 1. Effect of the percentage of melamine on the values of $RTlnV_n(T)$ of different adsorbed organic solvents at various temperatures: T = 453.15 K (**a**), T = 463.15 K (**b**), T = 473.15 K (**c**), and variations in $\Delta G_a(\text{-}CH_2\text{-})$ of n-alkanes adsorbed on solid surfaces as a function of temperature (**d**).

The curves presented in Figure 1 show an important variation in $RTlnV_n(T)$ of the various organic solvents as a function of temperature and the percentage of melamine on the porous polymer Dowex L-285. It seems that these variations were stabilized after 3% of melamine. Figure 1d also shows a significant decrease in the values of ΔG_a(-CH_2-) of n-alkanes for 1% and 4% of melamine; however, a slight decrease was observed in the two cases of 2% and 3% of melamine (Figure 1d). The deviation between these results was certainly due to the closer values of $RTlnV_n(T)$ (Figure 1a–c) of the adsorbed n-alkane solvents for 2% and 3% of melamine that implied closer values of ΔG_a(-CH_2-) at different temperatures. These observations show that 1% of melamine had a screening effect on the surface of the copolymer which gave constant values of ΔG_a(-CH_2-) until a melamine percentage lower than 4%. An increase in the surface thermodynamic parameters was observed at 4% for the various temperatures, proving an important effect of the melamine on the surface properties of the copolymer.

However, the variations in $RTlnV_n(T)$ of the different probes adsorbed on solid materials alone cannot describe the polar and dispersive free energies of adsorption. In the next sections, a new methodology was applied to better determine the London dispersive surface energy and the surface thermodynamic parameters of interaction of the examined porous polymers with the model organic molecules.

3.2. London Dispersive Surface Energy of Dowex L-285 with Different Melamine Percentages

The new expressions of the surface area $a(T)$ of organic solvents were obtained using the Hamieh thermal model [19–23]. The slopes of straight lines representing the variations in $RTlnV_n(T)$ of n-alkanes adsorbed on Dowex L-285 with different percentages of melamine as a function of $2\mathcal{N}a(T)\left(\gamma_l^d\right)^{1/2}$ using the London dispersive surface energy $\gamma_l^d(T)$ of n-alkanes [19–23], gave the values of the London dispersive surface energy $\gamma_s^d(T)$ of the various porous polymers for the different temperatures. The variations in the London dispersive surface energy of materials when the temperature and the percentage of melamine varied are presented in Figure 2. A linear decrease in $\gamma_s^d(T)$ was observed for all materials when the temperature increased (Figure 2a). The highest values of $\gamma_s^d(T)$ were obtained for the copolymer Dowex L-285 without any addition of melamine. An important difference in the behavior of different materials was observed in Table 1, showing different values of $\gamma_s^d(T)$ of Dowex L-285 modified by melamine percentages, the London dispersive surface entropy ε_s^d, the extrapolated values of London dispersive surface energy at 0 K and 298.15 K, and the temperature maximum T_{Max}.

Table 1. Linear expressions of $\gamma_s^d(T)$ of Dowex L-285 modified by different percentages of melamine, regression coefficients, London dispersive surface entropy ε_s^d, extrapolated values of London dispersive surface energy at 0 K and 298.15 K, and the temperature maximum T_{Max}.

Solid Material	$\gamma_s^d(T)$ **(mJ/m²)**	**R²**	$\varepsilon_s^d = d\gamma_s^d/dT$ **(mJ m⁻² K⁻¹)**	γ_s^d **(T = 0 K) (mJ/m²)**	γ_s^d **(T = 298.15 K) (mJ/m²)**	T_{Max} **(K)**
Dowex L-285	$\gamma_s^d(T) = -0.835\,T + 482.43$	0.9980	−0.835	482.43	233.47	577.8
1% Melamine	$\gamma_s^d(T) = -0.907\,T + 496.21$	0.9972	−0.907	496.21	225.79	547.1
2% Melamine	$\gamma_s^d(T) = -0.656\,T + 341.59$	0.9590	−0.656	341.59	146.12	521.0
3% Melamine	$\gamma_s^d(T) = -0.827\,T + 439.96$	0.9608	−0.827	439.96	193.51	532.3
4% Melamine	$\gamma_s^d(T) = -0.876\,T + 473.64$	0.9735	−0.876	473.64	212.40	540.6

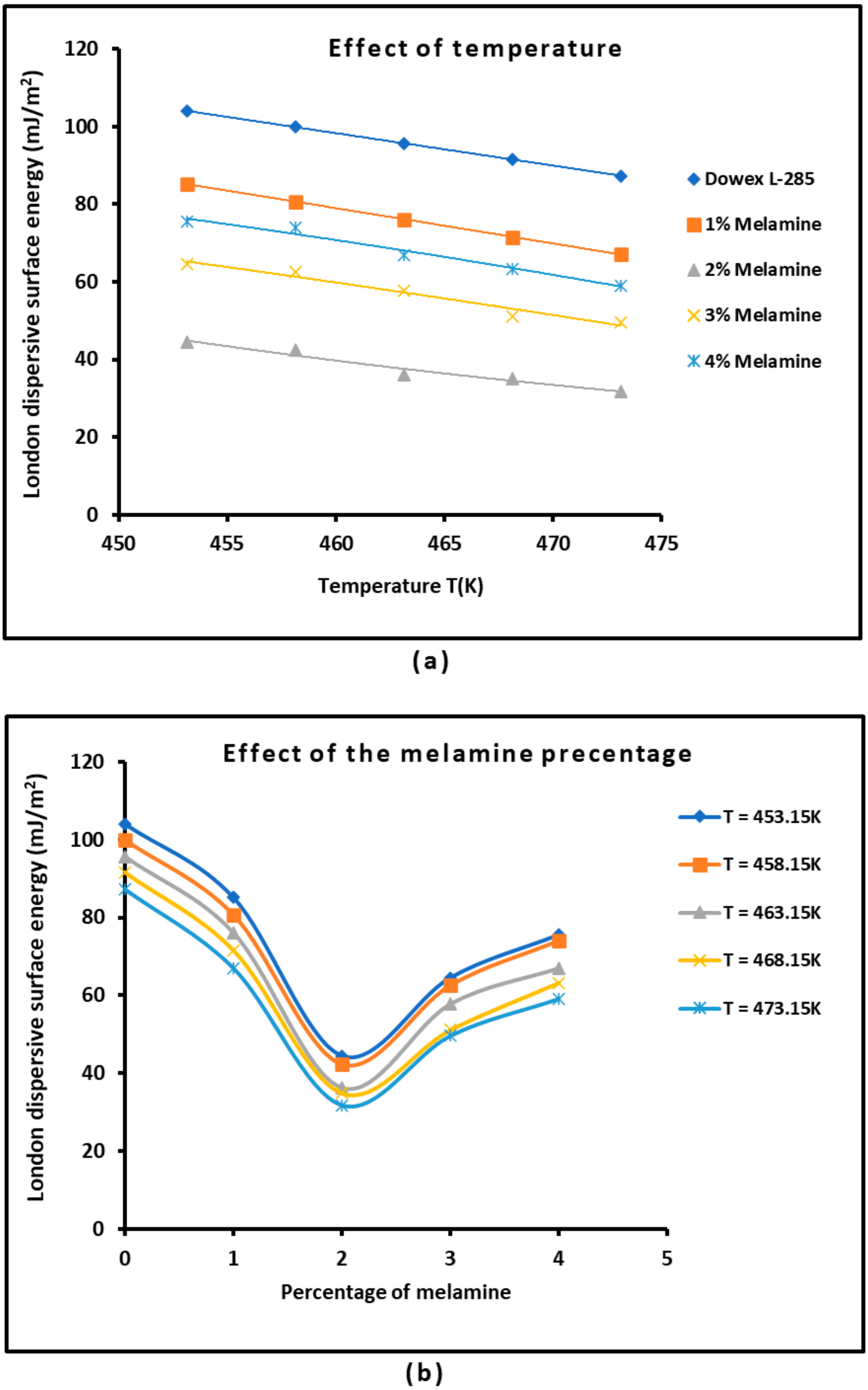

Figure 2. Variations in the London dispersive surface energy of materials as a function of the temperature (**a**) and the percentage of melamine (**b**).

A minimum in the different values of ε_s^d, $\gamma_s^d(T = 0\ \mathrm{K})$, $\gamma_s^d(T = 298.15\ \mathrm{K})$, and T_{Max} was obtained for 2% of melamine, proving that there was a change in the surface groups of the copolymer due to the effect of this minimum percentage on the different surface parameters of Dowex L-285. Figure 2b highlights the presence of such a minimum of melamine. The obtained curves of γ_s^d of solid materials presented in Figure 2b at different temperatures clearly show a minimum of γ_s^d corresponding to 2% of melamine.

The values of extrapolated London dispersive surface energy at room temperature were limited to 140 to 230 mJ/m^2 for the different melamine percentages. In a recent paper [45], $\gamma_s^d = 290$ mJ/m^2 was obtained using the Dorris–Gray (DG) method and $\gamma_s^d = 220$ mJ/m^2, applying the linear free-energy relationship (LFER) coupled with the Dorris–Gray calculation (DG–LFER) for the same copolymer Dowex L-285 modified with 1% melamine, while our new methodology gave $\gamma_s^d = 225.8$ mJ/m^2. Our results were based on the use of the Hamieh thermal model to determine the London dispersive surface energy. This thermal model was proved to be the most accurate method, because it takes into consideration the effect of the temperature on the surface area of organic molecules needed for the evaluation of London dispersive surface energy. The deviation percentage of another method, *X*, was calculated using the following relation:

$$Deviation\ Percentage\ of\ method\ X = \frac{\gamma_s^d(Method\ X) - \gamma_s^d(Hamieh\ Method)}{\gamma_s^d(Hamieh\ Method)} \times 100 \quad (18)$$

Using the above relation, one can deduce a deviation, in the case of DG method, of 31.8%. This large deviation is due to the DG method used by Gustov that did not take into account the temperature effect on the surface area of methylene group. However, a deviation of 2.6% was obtained using DG–LFER method. The value obtained by our new method was very close to that obtained by Guskov et al. using the DG–LFER calculation. However, the advantage of the new methodology, using the Hamieh thermal model, is to give the expressions of $\gamma_s^d(T)$ for the different percentages of melamine. For Dowex L-285 modified by 1% of melamine, the following relation is obtained:

$$\gamma_s^d(T) = -0.907\ T + 496.21 \quad (19)$$

The obtained values of $\gamma_s^d(T)$ of the styrene–divinylbenzene copolymer as a function of temperature were correlated with the thermal conductivity *K* of this copolymer. Indeed, Yamamoto and Kambe [46] determined the thermal conductivity of this material by the following relation:

$$K\left(\mathrm{mW} \times \mathrm{K}^{-1}\mathrm{m}^{-1}\right) = 0.897T(\mathrm{K}) - 155.28 \quad (20)$$

The results in Table 1 and Equation (20) led to the expression of the thermal conductivity $K(T)$ as a function of γ_s^d:

$$K\left(\mathrm{mW} \times \mathrm{K}^{-1}\mathrm{m}^{-1}\right) = -1.074\ \gamma_s^d\left(\mathrm{mJ} \times \mathrm{m}^{-2}\right) + 362.97 \quad (21)$$

Equation (21) clearly shows that the thermal conductivity *K* of Dowex L-285 decreased when the London dispersive surface energy increased or when the temperature decreased. This study confirmed the results, obtained in a recent paper [47], of the presence of a strong relationship between the thermal conductivity of some graphene and carbon materials and their London dispersive surface energy.

3.3. Polar Free Interaction Energy of Dowex L-285 Modified by Melamine with the Polar Probes

The free polar energy $-\Delta G_a^p(T)$ of adsorption of polar organic probes adsorbed on the different solid materials was determined, against temperature, using our new approach, Equations (5)–(8), and Table S1. The obtained results are presented in Table S2.

The curves of $-\Delta G_a^p(T)$ of the various polar organic probes adsorbed on Dowex L-285, drawn in Figure 3, as a function of temperature, show linear variations in the various melamine percentages. The obtained straight lines of the $-\Delta G_a^p(T)$ function of the temperature easily led to the polar enthalpy ($-\Delta H_a^p$) and entropy ($-\Delta S_a^p$) values of the adsorbed polar solvents.

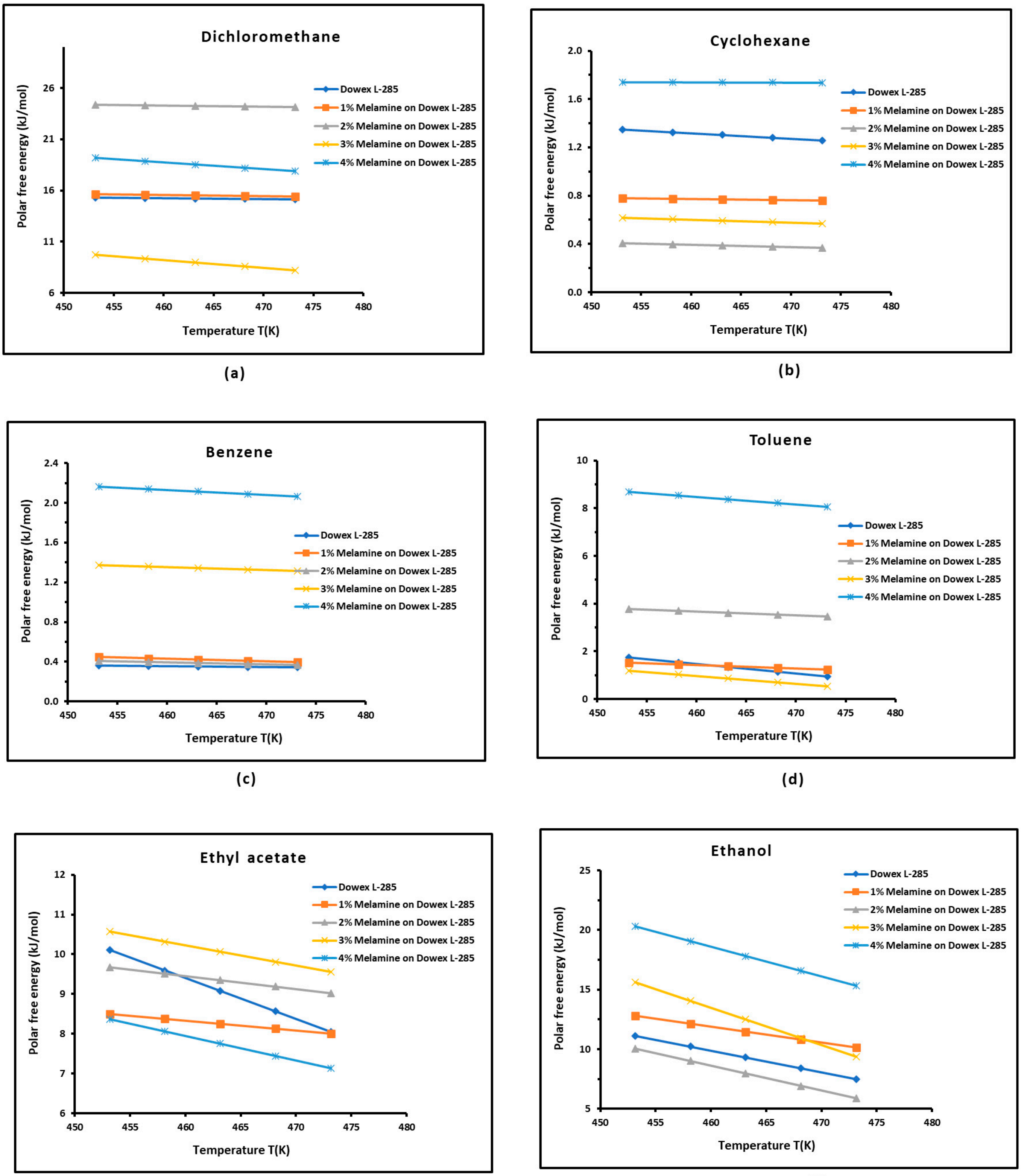

(a) (b) (c) (d) (e) (f)

Figure 3. *Cont.*

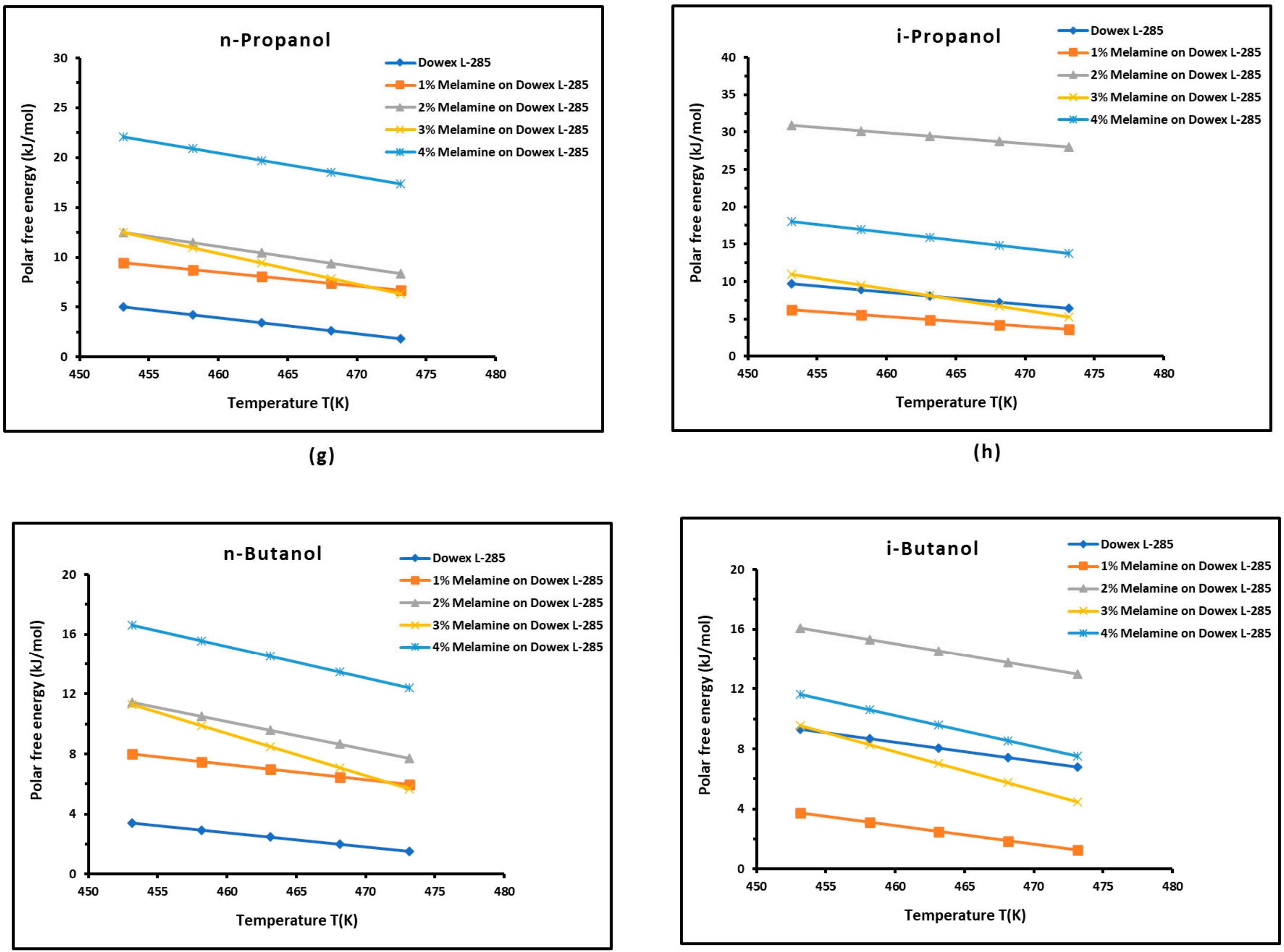

(g) **(h)**

(i) **(j)**

Figure 3. Evolution of the free polar energy $\left[-\Delta G_a^p(T)\right]$ of the various polar organic probes adsorbed on the different solid materials as a function of temperature for different melamine percentages. (**a**) Dichloromethane, (**b**) cyclohexane, (**c**) benzene, (**d**) toluene, (**e**) ethyl acetate, (**f**) ethanol, (**g**) *n*-propanol, (**h**) *i*-propanol, (**i**) *n*-butanol, and (**j**) *i*-butanol.

Several conclusions can be deduced from the curves in Figure 3:

- The free polar energies, $-\Delta G_a^p(T)$, of interaction between the solids and the organic solvents can be globally classified in increasing order of interaction energy with the various polar probes at all temperatures: cyclohexane < benzene < toluene < ethyl acetate < *i*-butanol < *n*-butanol < ethanol < *n*-propanol < dichloromethane < *i*-propanol.
- The highest free interaction energy was obtained for 4% melamine on Dowex L-285 for the following polar molecules in increasing order: cyclohexane < benzene < toluene < *n*-butanol < ethanol < *n*-propanol.
- However, a maximum of free interaction energy was observed for 2% melamine on Dowex L-285 for the other polar solvents such as dichloromethane, i-propanol, and i-butanol.
- It was proved that the alcohol molecules exchanged the maximum free interaction energy with the various solid surfaces, and especially with 4% melamine, while the minimum interaction was observed in the case of adsorption on Dowex L-285.
- The above results show that the modification of the copolymer Dowex L-285 by melamine increased the polar free interaction.

The above results were confirmed by the curves of $-\Delta G_a^p$ presented in Figure 4 as a function of the percentage of melamine on Dowex L-285 at different temperatures, where the maximum of the free interaction energy is shown for all polar solvents. Different non-linear variations in the free interaction energy were observed for the various polar molecules when the melamine percentage increased, but with a global increasing tendency of $-\Delta G_a^p$.

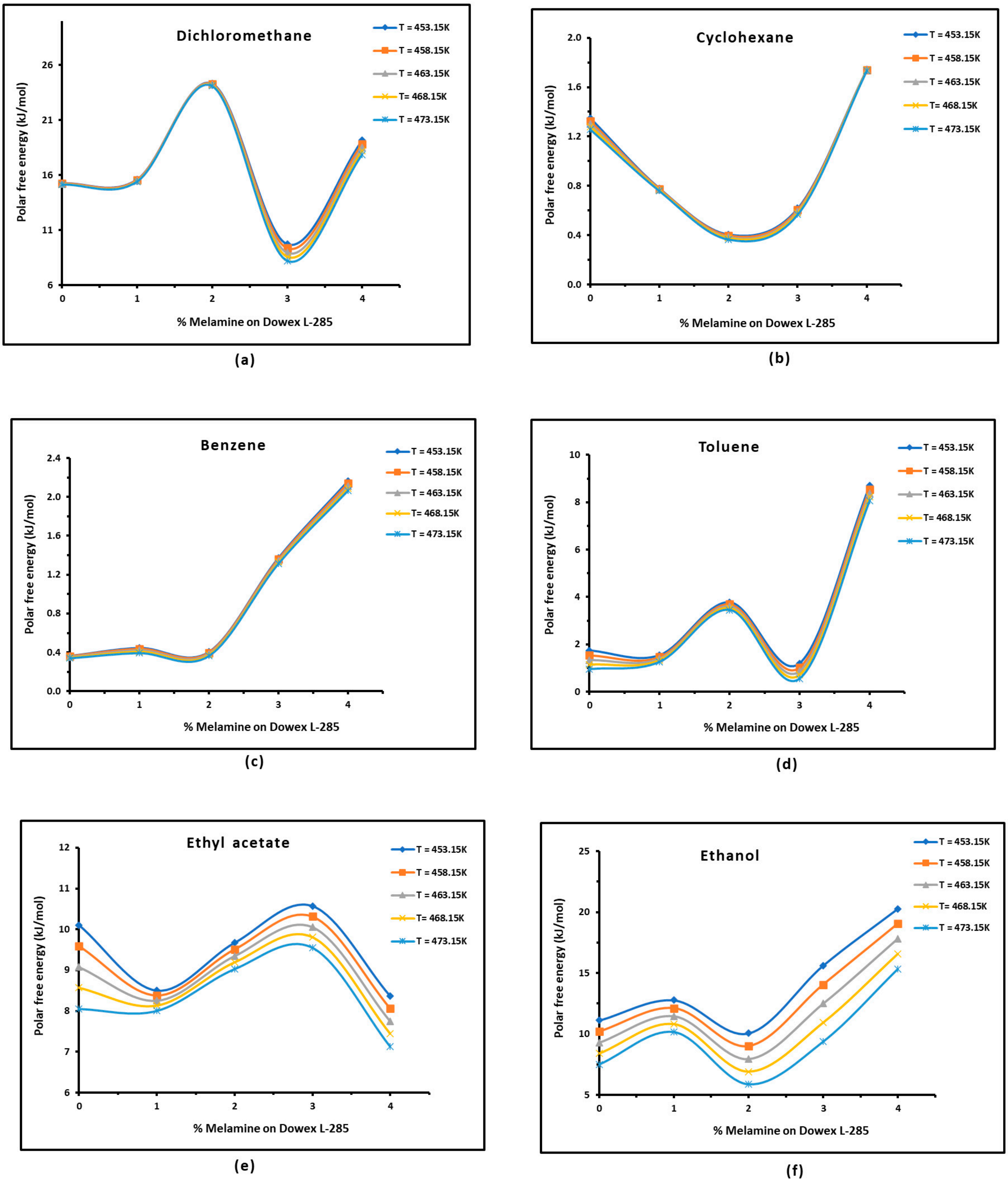

(a) (b) (c) (d) (e) (f)

Figure 4. *Cont.*

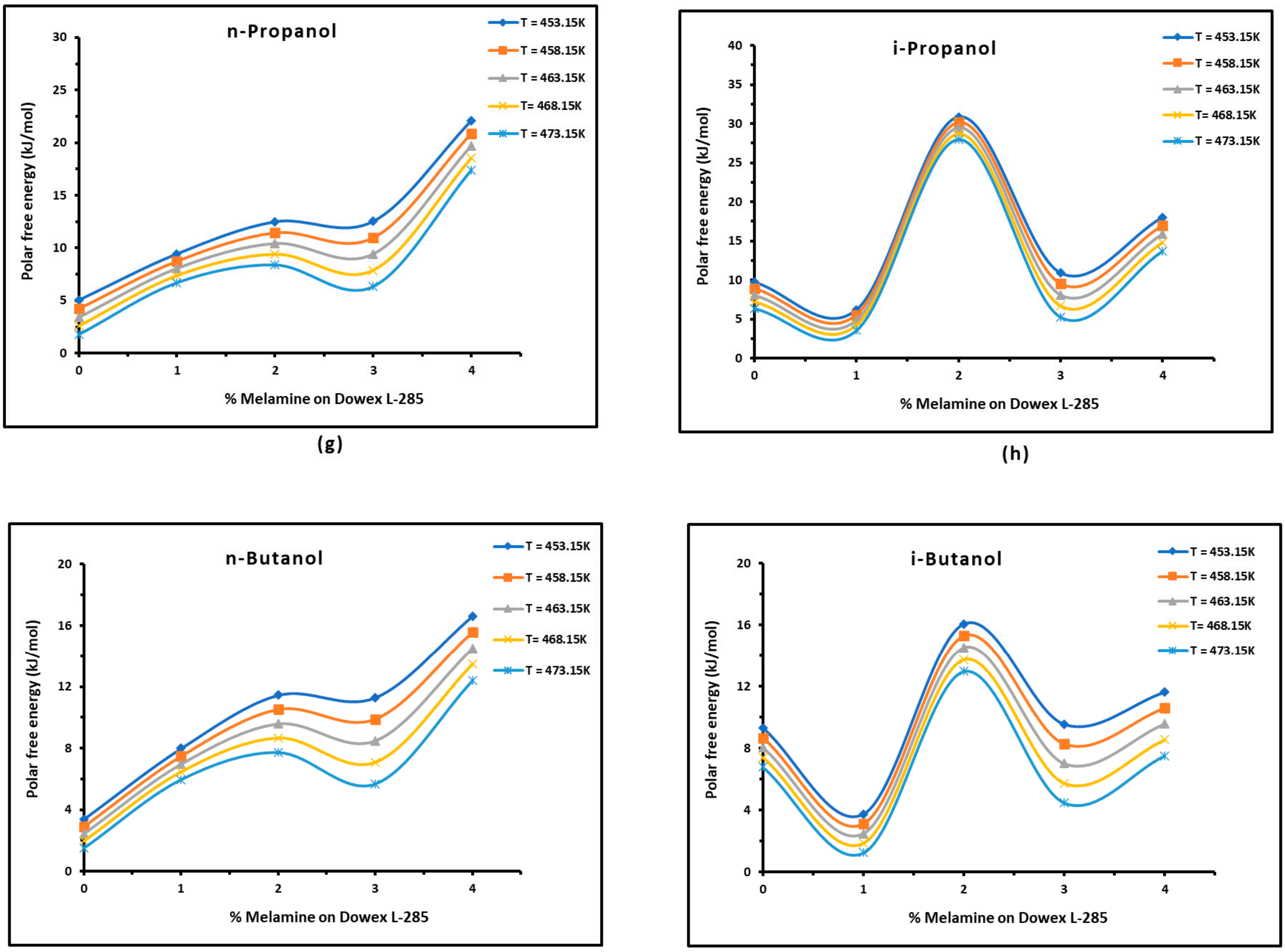

(g) (h) (i) (j)

Figure 4. Variations in the free polar energy $\left[-\Delta G_a^p(T)\right]$ of polar organic probes adsorbed on the different solid materials as a function of melamine percentage on Dowex L-285 at various temperatures. (**a**) Dichloromethane, (**b**) cyclohexane, (**c**) benzene, (**d**) toluene, (**e**) ethyl acetate, (**f**) ethanol, (**g**) *n*-propanol, (**h**) *i*-propanol, (**i**) *n*-butanol, and (**j**) *i*-butanol.

In order to better understand the polar behavior of the different solid surfaces, it was necessary to determine the surface polar enthalpy and the entropy of adsorption, as well as the Lewis acid–base constants of the solid materials. This is developed in the next section.

3.4. Polar Enthalpy and Entropy of Adsorption, and Lewis Acid–Base Parameters of Dowex L-285 Modified by Melamine

The polar enthalpy $\left(-\Delta H_a^p\right)$ and entropy $\left(-\Delta S_a^p\right)$ of the polar solvents adsorbed on the copolymer Dowex L-285 modified by different melamine percentages, were deduced from the variations in $-\Delta G_a^p(T)$ using Table S2, Figure 3, and Equation (9). The curves in Figure 5 show that the approximate linear variations in $\left(\frac{-\Delta H_a^p}{AN'}\right)$ and $\left(\frac{-\Delta S_a^p}{AN'}\right)$ versus $\left(\frac{DN'}{AN'}\right)$ of the polar solvents adsorbed on the different solid materials led to the values of the Lewis enthalpic K_A and K_D and entropic ω_A and ω_D acid–base constants of Dowex L-285 with different melamine percentages. The results are presented in Table 2 and clearly show an amphoteric behavior of the different solid surfaces with a Lewis basicity higher than their Lewis acidity for all solid substrates.

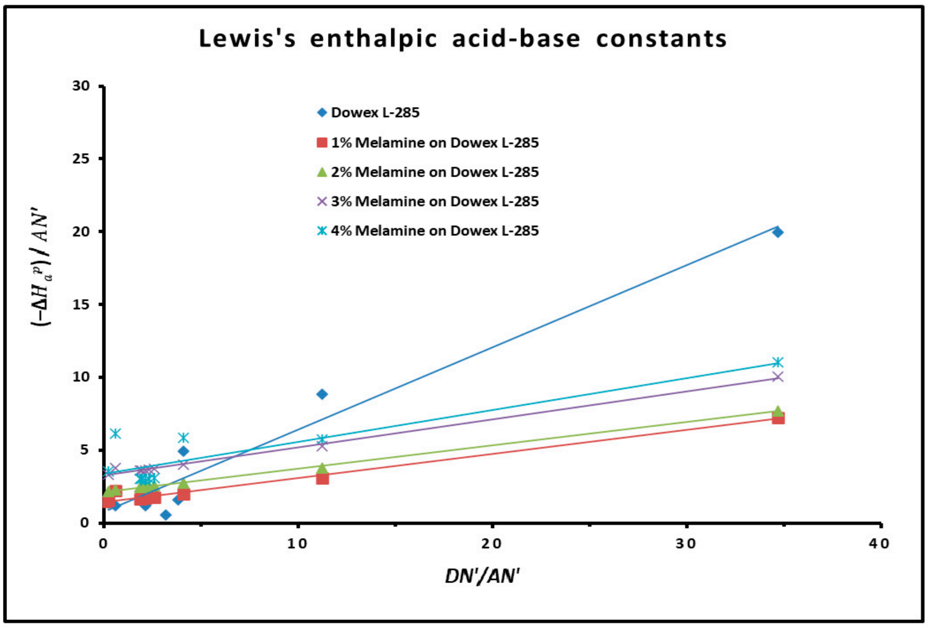

(a)

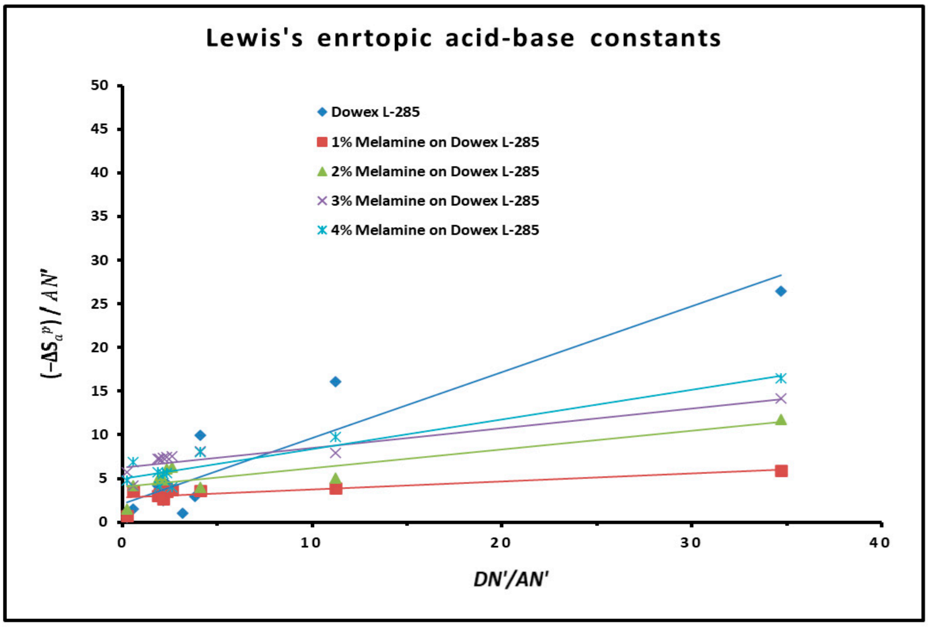

(b)

Figure 5. Variations in $\left(\frac{-\Delta H_a^p}{AN'}\right)$ and $\left(\frac{-\Delta S_a^p}{AN'}\right)$ against $\left(\frac{DN'}{AN'}\right)$ of polar solvents adsorbed on Dowex L-285 modified by different percentages of melamine.

The values of the Lewis acid and base constants of different materials were obtained using Equation (10) and Figure 5. The slopes of straight lines of $\left(\frac{-\Delta H_a^p}{AN'}\right)$ and $\left(\frac{-\Delta S_a^p}{AN'}\right)$ against $\left(\frac{DN'}{AN'}\right)$ determined the Lewis acid constants K_A and ω_A, while the ordinates at origin led to the Lewis base constants K_D and ω_D. The results in Table 2 show that Dowex L-285 exhibited the highest acid character, whereas the copolymer modified by 4% of melamine had the highest basicity. The results presented in Figure 6 show that the basicity of solid materials largely increased when the melamine percentage increased, while a brutal decrease in the acidity was observed when Dowex L-285 was modified by 1% of melamine. A slight increase in acidity was found when the melamine percentage passed from 2% to 4%. The same conclusions were observed for the entropic acid–base constants. The total acid–base parameters $S_K = K_A + K_D$ and $S_K = \omega_A + \omega_D$ are given in Table 2. It was proved that the total acidity–basicity increased when the melamine percentage increased. It seemed that this continued for all acid–base parameters of solid surfaces after 3% of melamine. In fact, the presence of six nitrogen atoms in the supramolecular structure of melamine increased its donor interaction of electrons when added to the structure of styrene–divinylbenzene copolymer. This increased the basicity of Dowex L-285 when the melamine percentage increased, while the Lewis acidity decreased because of the strong basic sites of melamine that certainly interacted with the acidic sites of the copolymer by decreasing the total acidity of the solid materials.

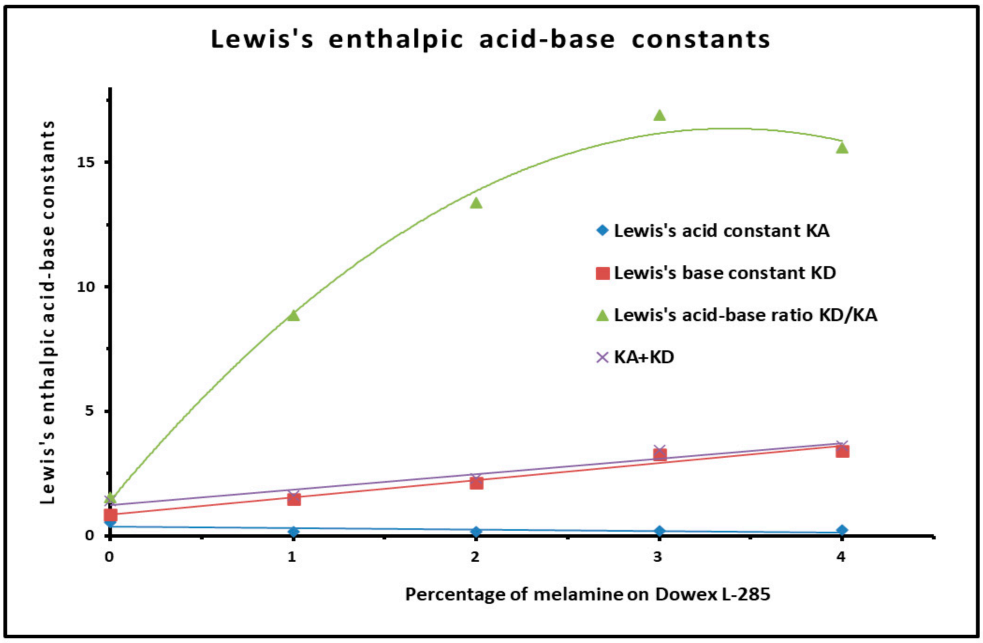

(a)

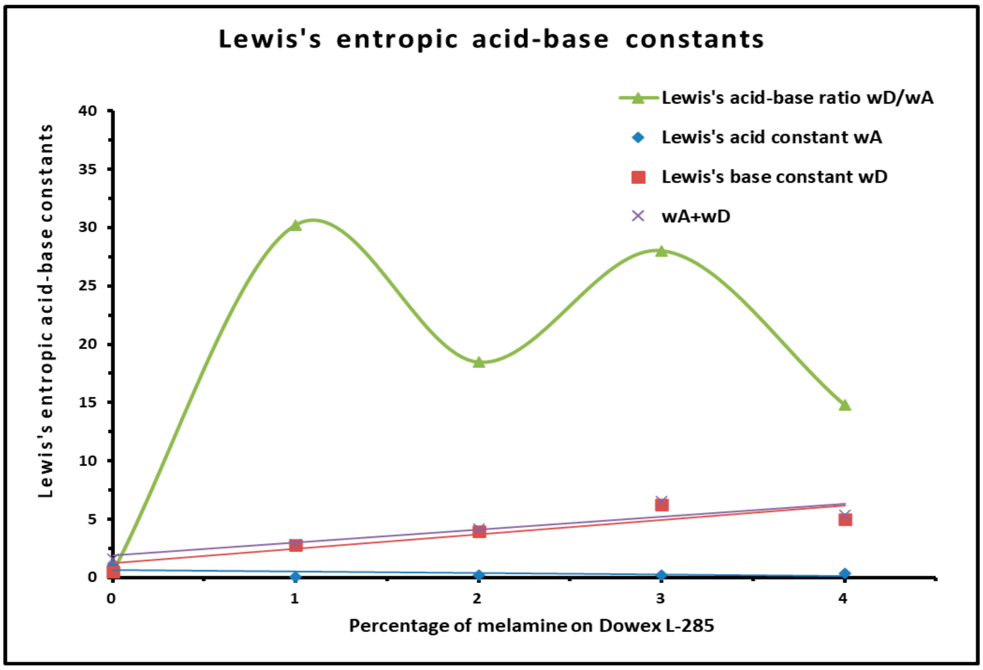

(b)

Figure 6. (**a**,**b**) Curves of the Lewis enthalpic and entropic acid–base constants K_A, K_D, ω_A, and ω_D; the acid–base ratios; and the corresponding parameters $S_K = K_A + K_D$ and $S_K = \omega_A + \omega_D$ as a function of melamine percentage.

Table 2. Values of the Lewis acid–base constants K_A, K_D, ω_A, and ω_D; the acid–base ratios; and the linear regression coefficient R^2 relative to Dowex L-285, modified by different melamine percentages with the corresponding parameters S_K = K_A + K_D and S_K = ω_A + ω_D.

Material	K_A	K_D	K_D/K_A	$K_A + K_D$	**R^2**	$10^{-3}\omega_A$	$10^{-3}\omega_D$	ω_D/ω_A	$10^{-3}(\omega_A + \omega_D)$	**R^2**
Dowex L-285	0.550	0.844	1.53	1.393	0.999	1.05	0.55	0.5	1.59	0.9968
1% Melamine on Dowex L-285	0.164	1.455	8.85	1.620	0.9783	0.09	2.81	30.2	2.90	0.9316
2% Melamine on Dowex L-285	0.160	2.137	13.38	2.297	0.9989	0.22	4.00	18.5	4.21	0.9520
3% Melamine on Dowex L-285	0.193	3.263	16.90	3.456	0.9938	0.22	6.30	28.0	6.52	0.9695
4% Melamine on Dowex L-285	0.218	3.401	15.58	3.619	0.9276	0.34	5.00	14.8	5.34	0.9702

3.5. Polar Acid–Base Surface Energies of Dowex L-285 Modified by Melamine

The different polar surface energies, such as the polar acid γ_s^+ and base γ_s^- surface energies of Dowex L-285 modified by different melamine percentages were determined using the method of Van Oss et al. [44]. To do that, the free polar energy $-\Delta G_a^{sp}(T)$ of the different polar molecules, given in Table 3, was used to determine the values of γ_s^+ and γ_s^- at different temperatures, knowing the values of the polar acid γ_l^+ and base γ_l^- surface energies of two chosen polar solvents such as dichloromethane and ethyl acetate molecules.

Table 3. Values of $-\Delta G_a^p(T)$ (inkJ/mol) for dichloromethane and ethyl acetate adsorbed on Dowex L-285 modified with different melamine percentages at different temperatures.

Dichloromethane					
T(K)	Dowex L-285	1% Melamine	2% Melamine	3% Melamine	4% Melamine
453.15	15.274	15.609	24.349	9.737	16.294
458.15	15.239	15.559	24.294	9.352	16.452
463.15	15.204	15.509	24.239	8.967	16.012
468.15	15.169	15.459	24.184	8.582	15.989
473.15	15.134	15.409	24.129	8.197	12.318
Ethyl Acetate					
T(K)	Dowex L-285	1% Melamine	2% Melamine	3% Melamine	4% Melamine
453.15	10.106	8.503	9.667	10.567	39.887
458.15	9.593	8.378	9.507	10.314	38.842
463.15	9.079	8.253	9.347	10.060	37.077
468.15	8.566	8.128	9.187	9.807	35.814
473.15	8.052	8.003	9.027	9.553	30.163

Using Equations (13) and (15), the values of $-\Delta G_a^{sp}(T)$ in Table 3, and the Hamieh thermal model, we obtained the values of γ_s^+ and γ_s^- of the various solid surfaces as a function of temperature. The polar acid–base surface energy $\gamma_s^{AB} = \gamma_s^p$ was then deduced from the relation $\gamma_s^p = 2\sqrt{\gamma_s^+\gamma_s^-}$. This led to the total surface energy $\gamma_s^{tot.}$ of the different solid surfaces using the relation $\gamma_s^{tot.} = \gamma_s^d + \gamma_s^p$.

The variations in $\gamma_s^+(T)$, $\gamma_s^-(T)$, $\gamma_s^{AB}(T)$, $\gamma_s^d(T)$, and $\gamma_s^{tot.}(T)$ of Dowex L-285 with different percentages of melamine are given in Table S3. Figure 7 gives the linear variations in polar surface energy components of Dowex L-285 modified by different melamine percentages as a function of temperature. The results show that the highest polar surface energy values were obtained with the Lewis base surface energy for all materials, while the lowest values were highlighted with the Lewis acid surface energy, confirming the highest basic character of Dowex L-285 at different melamine percentages. Furthermore, the maximum values of the Lewis base surface energy and the polar acid–base surface energy were obtained when using Dowex L-285 modified by 2% of melamine, followed by that of 4% of melamine.

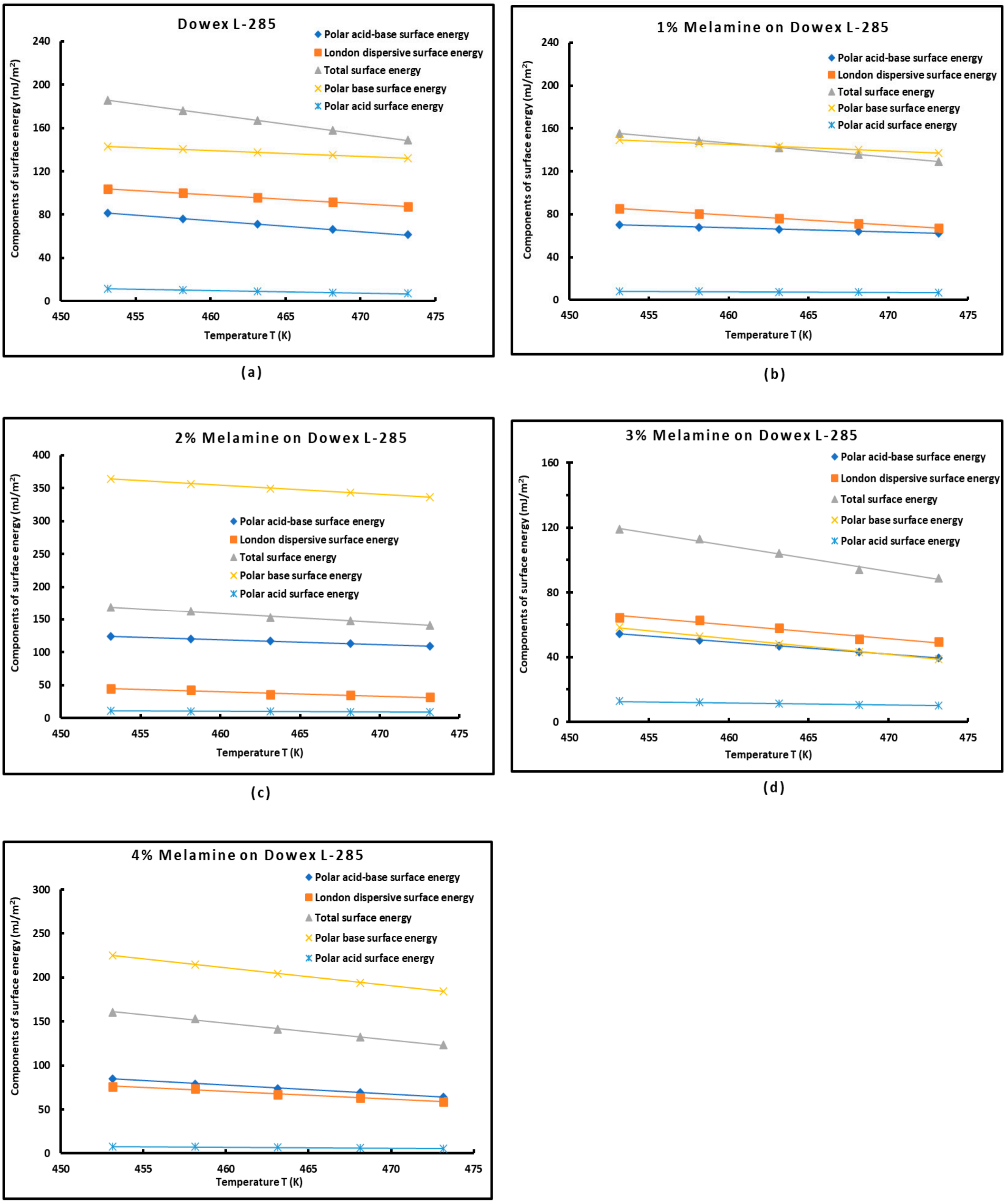

(a) (b) (c) (d) (e)

Figure 7. *Cont.*

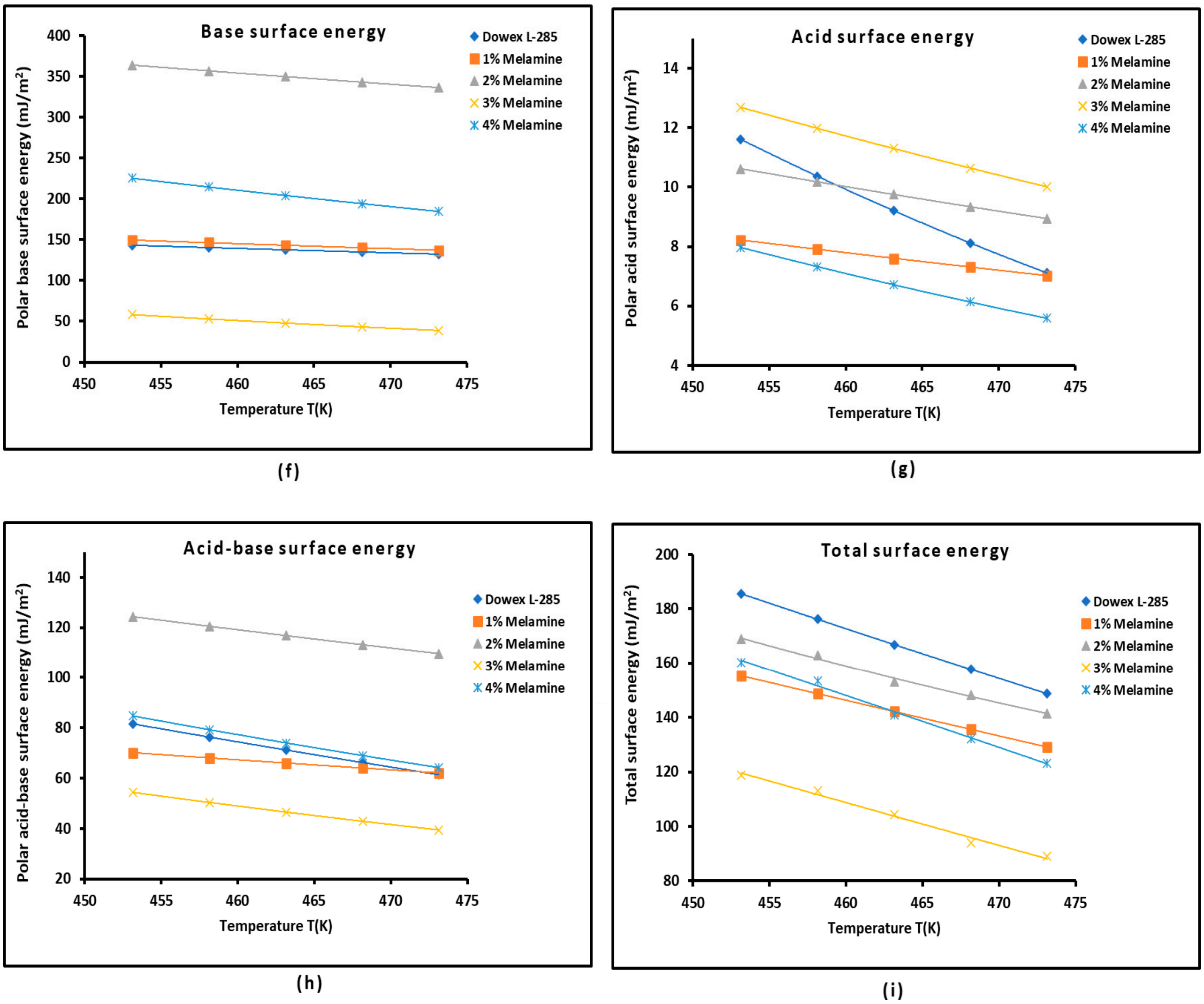

(f) (g)

(h) (i)

Figure 7. Variations in acid and base surface energy components, and total energy (in mJ/m^2) of Dowex L-285 modified by different melamine percentages as a function of temperature: Dowex L-285 (**a**), 1% melamine (**b**), 2% melamine (**c**), 3%melamine (**d**), 4% melamine (**e**), base surface energy (**f**), acid surface energy (**g**), acid–base surface energy (**h**), and total surface energy (**i**).

By applying the Hamieh thermal model to determine the values of the surface area of organic molecules adsorbed on the different solid surfaces as a function of temperature and the results in Table S3 and Figure 7, Figure 8 shows the variations in the polar surface energy of the adsorbed polar probes against the temperature using the Fowkes relation [43]. The highest values of the polar surface energy were obtained with dichloromethane and ethanol adsorbed on the various solid materials, whereas, the lowest values were obtained in the case of adsorption of cyclohexane and benzene. These results are in perfect agreement with the polarity of the above organic molecules.

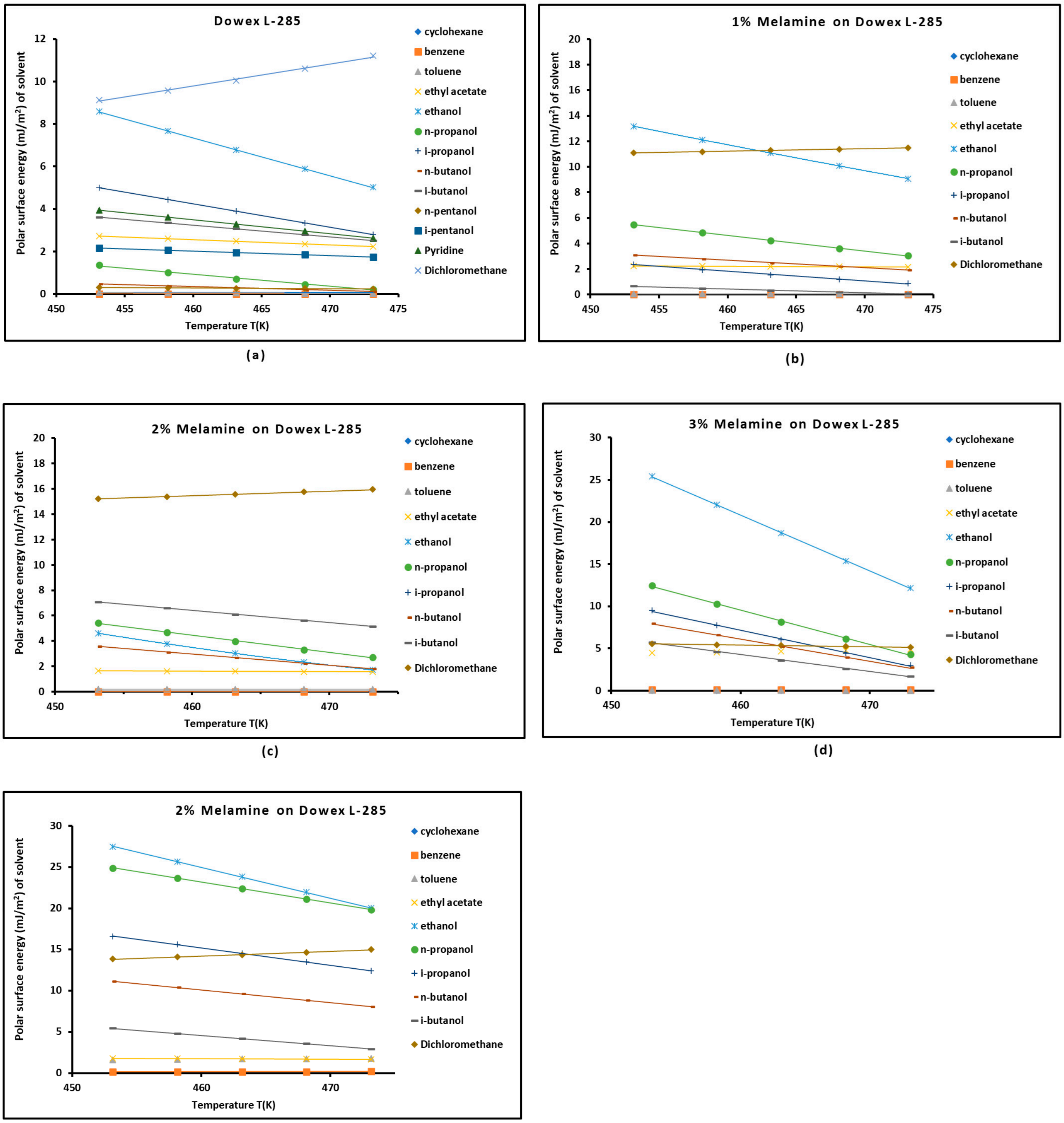

(a) (b) (c) (d) (e)

Figure 8. Variations in polar surface energy (in mJ/m^2) of the different polar solvents adsorbed on Dowex L-285 modified by different melamine percentages as a function of temperature: Dowex L-285 (**a**), 1% melamine (**b**), 2% melamine (**c**), 3% melamine (**d**), and 4% melamine (**e**).

3.6. Determination of the Average Separation Distance H

The separation distance H between the organic molecules and the solid surfaces was determined as a function of the temperature, using Equations (7) and (8) and the previous experimental results. The obtained curves are plotted in Figure 9. It was observed that the separation distance H increased when the temperature increased proving the effect of the thermal agitation on the separation distance between molecules and solid substrates. The results show that the separation distance was between 5.5 Å and 6.1 Å, with the highest value in the case of 2% of melamine.

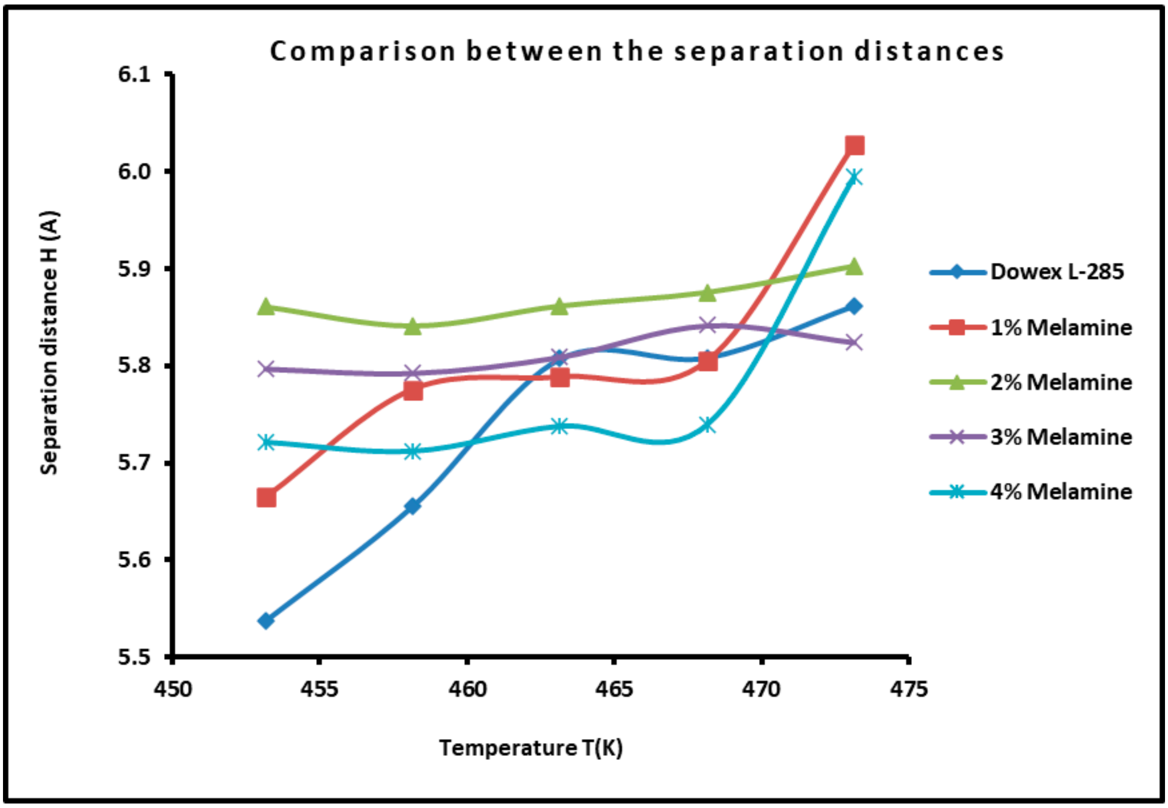

Figure 9. Evolution of the separation distance $H(T)$ (in Å) between the organic solvents and Dowex L-285, modified by melamine supramolecule, as a function of the temperature.

4. Conclusions

The surface thermodynamic properties of styrene–divinylbenzene copolymer (Dowex L-285) modified by a supramolecular structure of melamine at different percentages were characterized using the inverse gas chromatography at infinite dilution. The new methodology based on the Hamieh thermal model was used for accurate determination of the London dispersive surface energy of the different materials as a function of the temperature and the melamine percentage. A linear decrease in $\gamma_s^d(T)$ in the London dispersive surface energy of materials was noticed when the temperature increased, with the highest value obtained for the copolymer Dowex L-285. The results show an important difference in the behavior of different materials when the melamine percentage varied. This study highlighted a linear correlation between the thermal conductivity of the styrene–divinylbenzene copolymer and its London dispersive surface energy, confirming similar relationships previously obtained with graphene and carbon materials.

The application of our new methodology using the London dispersion interaction on the styrene–divinylbenzene copolymer modified by melamine led to the determination of the polar free energy, enthalpy, and entropy of adsorption of polar solvents on the various solid surfaces, as well the Lewis acid–base constants. It was proved that all materials used exhibited basic behavior that was largely higher than their acid behavior and the basic character increased with the melamine percentage in good agreement with the increase in nitrogen atom number at the surface of solid materials. The determination of the various components of polar acid and base surface energies of the different materials led to the conclusion that the highest polar surface energy values were obtained with the Lewis base surface energy for all materials, while the lowest values were obtained with the Lewis acid surface energy, confirming the highest basic character of Dowex L-285 at different melamine percentages. It was also shown that the maximum values of the Lewis base surface energy and the polar acid–base surface energy were obtained when using Dowex L-285 modified by 2% of melamine, which showed the highest separation distance between surface materials and organic solvents.

Supplementary Materials: The following supporting information can be downloaded at: https://www.mdpi.com/article/10.3390/chemistry6050050/s1. Table S1. Values of $RTlnVn$ (kJ/mol) of n-alkanes adsorbed on silica particles as a function of the temperature. Table S2. Variations in $\Delta G_a^{sp}(T)$ (kJ/mol) of different polar solvents adsorbed on Dowex L-285 and various melamine percentages as a function of temperature. Table S3. Values of $\gamma_s^+(T)$, $\gamma_s^-(T)$, $\gamma_s^{AB}(T)$, $\gamma_s^d(T)$, and $\gamma_s^{tot.}(T)$ of Dowex L-285 and the different percentages of melamine on the copolymer.

Author Contributions: Conceptualization, T.H. and V.Y.G.; methodology, T.H.; software, T.H.; validation, T.H. and V.Y.G.; formal analysis, T.H. and V.Y.G.; investigation, T.H. and V.Y.G.; resources, V.Y.G.; data curation, V.Y.G.; writing—original draft preparation, T.H.; writing—review and editing, T.H.; visualization, T.H. and V.Y.G.; project administration, T.H. and V.Y.G.; funding acquisition, V.Y.G. All authors have read and agreed to the published version of the manuscript.

Funding: This research received no external funding.

Data Availability Statement: The data presented in this study are available in the article and Supplementary Materials.

Acknowledgments: We thank Sami Tlais for his kind financial support relative to the publication fees.

Conflicts of Interest: The authors declare no conflicts of interest.

References

1. Gus'kov, V.Y.; Bilalova, R.V.; Kudasheva, F.K. Adsorption of organic molecules on a melamine-modified porous polymer. *Russ. Chem. Bull.* **2017**, *66*, 857–861. [CrossRef]
2. Zaitsev, S.Y.; Vereschetin, V.P.; Gromov, S.P.; Fedorova, O.A.; Alfimov, M.V.; Huesmann, H.; Möbius, D. Photosensitive supramolecular systems based on amphiphilic crown ethers. *Supramol. Sci.* **1997**, *4*, 519–524. [CrossRef]
3. Sukhareva, D.A.; Gus´kov, V.Y.; Karpov, S.I.; Kudasheva, F.K. Adsorption of organic molecules on the highly ordered MCM-41 sorbent modified by different amounts of melamine. *Russ. Chem. Bull.* **2017**, *66*, 958–962. [CrossRef]
4. Gainullina, Y.Y.; Gus'kov, V.Y.; Timofeeva, D.V. Polarity of Thymine and 6-Methyluracil-Modified Porous Polymers, According to Data from Inverse Gas Chromatography. *Russ. J. Phys. Chem.* **2019**, *93*, 2477–2481. [CrossRef]
5. Gus'kov, V.Y.; Shaihitdinova, Y.F.; Zil'berg, R.A.; Kraikin, V.A.; Maistrenko, V.N. Intermolecular interactions between polyarylenephthalides surface and organic compounds of different nature by inverse gas chromatography. *Sorpt. Chromatogr. Process* **2019**, *19*, 229–236. [CrossRef] [PubMed]
6. Onuchak, L.A.; Kapralova, T.S.; Kuraeva, Y.G.; Belousova, Z.P.; Stepanova, R.F. Sorption and selective chromatographic properties of isomer-selective composite sorbent based on a eutectic mixture of nematic liquid crystals and perbenzoylated β-cyclodextrin. *Russ. J. Phys. Chem. A* **2015**, *89*, 2304–2312. [CrossRef]
7. Lehn, J.-M. *Supramolecular Chemistry. Concepts and Perspectives*; VCH: Weinhiem, Germany, 1995; p. 271. [CrossRef]
8. Guo, F.; Cheung, E.Y.; Harris, K.D.M.; Pedireddi, V.R. Contrasting Solid-State Structures of Trithiocyanuric Acid and Cyanuric Acid. *Cryst. Growth Des.* **2006**, *6*, 846–848. [CrossRef]
9. Singh, U.P.; Kashyap, S.; Singh, H.J.; Mishra, B.K.; Roy, P.; Chakraborty, A. Effect of adenosine on the supramolecular architecture and activity of 5-fluorouracil. *J. Mol. Struct.* **2012**, *1014*, 47–56. [CrossRef]
10. Gus'kov, V.Y.; Gainullina, Y.Y.; Ivanov, S.P.; Kudasheva, F.K. Thermodynamics of organic molecule adsorption on sorbents modified with 5-hydroxy-6-methyluracil by inverse gas chromatography. *J. Chromatogr. A* **2014**, *1356*, 230–235. [CrossRef]
11. Breckenridge, W.H.; Ayles, V.L.; Wright, T.G. Evidence for Emergent Chemical Bonding in Au^+−Rg Complexes (Rg = Ne, Ar, Kr, and Xe). *J. Phys. Chem. A* **2008**, *112*, 4209–4214. [CrossRef]
12. Gus'kov, V.Y.; Ganieva, A.G.; Kudasheva, F.K. Monolayer capacity estimation by inverse gas chromatography at finite concentrations. *Colloids Surf. A* **2017**, *513*, 95–101. [CrossRef]
13. Gus'kov, V.Y.; Gainullina, Y.Y.; Ivanov, S.P.; Kudasheva, F.K. Properties of the surface of a porous polymer modified with 5-fluorouracil, according to data of gas chromatography. *Russ. J. Phys. Chem. A* **2014**, *88*, 1042–1046. [CrossRef]
14. Gus'kov, V.Y.; Gainullina, Y.Y.; Ivanov, S.P.; Kudasheva, F.K. Porous polymer adsorbents modified with uracil. *Prot. Met. Phys. Chem. Surf.* **2014**, *50*, 55–58. [CrossRef]
15. Gus'kov, V.Y.; Ivanov, S.P.; Khabibullina, R.A.; Garafutdinov, R.R.; Kudasheva, F.K. Gas chromatographic investigation of the properties of a styrene-divinylbenzene copolymer modified by 5-hydroxy-6-methyluracil. *Russ. J. Phys. Chem. A* **2012**, *86*, 475–478. [CrossRef]

16. Godlewski, S.; Tekiel, A.; Piskorz, W.; Zasada, F.; Prauzner-Bechcicki, J.S.; Sojka, Z.; Szymonski, M. Supramolecular ordering of PTCDA molecules: The key role of dispersion forces in an unusual transition from physisorbed into chemisorbed state. *ACS Nano* **2012**, *6*, 8536–8545. [CrossRef]
17. Dorris, G.M.; Gray, D.G. Adsorption of *n*-alkanes at zero surface coverage on cellulose paper and wood fibers. *J. Colloid Interface Sci.* **1980**, *77*, 353–362. [CrossRef]
18. Schultz, J.; Lavielle, L.; Martin, C. Propriétés de surface des fibres de carbone déterminées par chromatographie gazeuse inverse. *J. Chim. Phys.* **1987**, *84*, 231–237. [CrossRef]
19. Hamieh, T. Study of the temperature effect on the surface area of model organic molecules, the dispersive surface energy and the surface properties of solids by inverse gas chromatography. *J. Chromatogr. A* **2020**, *1627*, 461372. [CrossRef] [PubMed]
20. Hamieh, T.; Ahmad, A.A.; Roques-Carmes, T.; Toufaily, J. New approach to determine the surface and interface thermodynamic properties of H-β-zeolite/rhodium catalysts by inverse gas chromatography at infinite dilution. *Sci. Rep.* **2020**, *10*, 20894. [CrossRef]
21. Hamieh, T. New methodology to study the dispersive component of the surface energy and acid–base properties of silica particles by inverse gas chromatography at infinite dilution. *J. Chromatogr. Sci.* **2022**, *60*, 126–142. [CrossRef]
22. Hamieh, T. Inverse Gas Chromatography to Characterize the Surface Properties of Solid Materials. *Chem. Mater.* **2024**, *36*, 2231–2244. [CrossRef]
23. Hamieh, T. Some Irregularities in the Evaluation of Surface Parameters of Solid Materials by Inverse Gas Chromatography. *Langmuir* **2023**, *39*, 17059–17070. [CrossRef] [PubMed]
24. Hamieh, T. New Progress on London Dispersive Energy, Polar Surface Interactions, and Lewis's Acid–Base Properties of Solid Surfaces. *Molecules* **2024**, *29*, 949. [CrossRef] [PubMed]
25. Hamieh, T. London Dispersive and Lewis Acid-Base Surface Energy of 2D Single-Crystalline and Polycrystalline Covalent Organic Frameworks. *Crystals* **2024**, *14*, 148. [CrossRef]
26. London, F. The general theory of molecular forces. *Trans. Faraday Soc.* **1937**, *33*, 8–26. [CrossRef]
27. Conder, J.R.; Young, C.L. *Physical Measurements by Gas Chromatography*; John Wiley & Sons: Chichester, NY, USA, 1979; p. 632.
28. Sawyer, D.T.; Brookman, D.J. Thermodynamically based gas chromatographic retention index for organic molecules using salt-modified aluminas and porous silica beads. *Anal. Chem.* **1968**, *40*, 1847–1850. [CrossRef]
29. Liu, Y.; Gu, Y.; Wang, S.; Li, M. Optimization for testing conditions of inverse gas chromatography and surface energies of various carbon fiber bundles. *Carbon Lett.* **2023**, *33*, 909–920. [CrossRef]
30. Pal, A.; Kondor, A.; Mitra, S.; Thua, K.; Harish, S.; Saha, B.B. On surface energy and acid–base properties of highly porous parent and surface treated activated carbons using inverse gas chromatography. *J. Ind. Eng. Chem.* **2019**, *69*, 432–443. [CrossRef]
31. Schultz, J.; Lavielle, L.; Martin, C. The role of the interface in carbon fibre-epoxy composites. *J. Adhes.* **1987**, *23*, 45–60. [CrossRef]
32. Saint-Flour, C.; Papirer, E. Gas-solid chromatography. A method of measuring surface free energy characteristics of short glass fibers. 1. Through adsorption isotherms. *Ind. Eng. Chem. Prod. Res. Dev.* **1982**, *21*, 337–341. [CrossRef]
33. Saint-Flour, C.; Papirer, E. Gas-solid chromatography: Method of measuring surface free energy characteristics of short fibers. 2. Through retention volumes measured near zero surface coverage. *Ind. Eng. Chem. Prod. Res. Dev.* **1982**, *21*, 666–669. [CrossRef]
34. Donnet, J.-B.; Park, S.; Balard, H. Evaluation of specific interactions of solid surfaces by inverse gas chromatography. *Chromatographia* **1991**, *31*, 434–440. [CrossRef]
35. Chehimi, M.M.; Pigois-Landureau, E. Determination of acid–base properties of solid materials by inverse gas chromatography at infinite dilution. A novel empirical method based on the dispersive contribution to the heat of vaporization of probes. *J. Mater. Chem.* **1994**, *4*, 741–745. [CrossRef]
36. Brendlé, E.; Papirer, E. A New Topological Index for Molecular Probes Used in Inverse Gas Chromatography for the Surface Nanorugosity Evaluation. *J. Colloid Interface Sci.* **1997**, *194*, 207–216. [CrossRef]
37. Brendlé, E.; Papirer, E. A New Topological Index for Molecular Probes Used in Inverse Gas Chromatography. *J. Colloid Interface Sci.* **1997**, *194*, 217–224. [CrossRef] [PubMed]
38. Przybyszewska, M.; Krzywania, A.; Zaborski, M.; Szynkowska, M.I. Surface properties of zinc oxide nanoparticles studied by inverse gas chromatography. *J. Chromatogr. A* **2009**, *1216*, 5284–5291. [CrossRef] [PubMed]
39. Bakaoukas, N.; Sevastos, D.; Kapolos, J.; Koliadima, A.; Karaiskakis, G. Characterization of polymeric coatings in terms of their ability to protect marbles and clays against corrosion from sulfur dioxide by inverse gas chromatography. *Int. J. Polym. Anal. Charact.* **2013**, *18*, 401–4013. [CrossRef]
40. Rückriem, M.; Inayat, A.; Enke, D.; Gläser, R.; Einicke, W.-D.; Rockmann, R. Inverse gas chromatography for determining the dispersive surface energy of porous silica. *Colloids Surf. A Physicochem. Eng. Asp.* **2010**, *357*, 21–26. [CrossRef]
41. Gutmann, V. *The Donor-Acceptor Approach to Molecular Interactions*; Springer: New York, NY, USA, 1978; p. 279.
42. Riddle, F.L.; Fowkes, F.M. Spectral shifts in acid-base chemistry. Van der Waals contributions to acceptor numbers, Spectral shifts in acid-base chemistry. 1. van der Waals contributions to acceptor numbers. *J. Am. Chem. Soc.* **1990**, *112*, 3259–3264. [CrossRef]
43. Fowkes, F.M. Volume 1 Surface Chemistry and Physics. In *Surface and Interfacial Aspects of Biomedical Polymers*; Andrade, J.D., Ed.; Plenum Press: New York, NY, USA, 1985; pp. 337–372.
44. Van Oss, C.J.; Good, R.J.; Chaudhury, M.K. Additive and nonadditive surface tension components and the interpretation of contact angles. *Langmuir* **1988**, *4*, 884. [CrossRef]

45. Gus'kov, V.Y.; Gainullina, Y.Y.; Gabdulmanova, A.F.; Gareeva, A.N. Dispersive surface free energy of adsorbents modified by supramolecular structures of heterocyclic compounds. *Chim. Techno Acta* **2024**, *11*, 202411210. [CrossRef]
46. Yamamoto, O.; Kambe, H. Thermal conductivity of cross-linked polymers. A comparison between measured and calculated thermal conductivities. *Polym. J.* **1971**, *2*, 623–628. [CrossRef]
47. Hamieh, T. Thermal Surface Properties, London Dispersive and Polar Surface Energy of Graphene and Carbon Materials Using Inverse Gas Chromatography at Infinite Dilution. *Molecules* **2024**, *29*, 2871. [CrossRef] [PubMed]